Solar Electric Propulsion Asteroid Belt Mission

L. E. SCHWAIGER* AND J. M. SHOLLENBERGER JR.†
North American Rockwell Corporation, Seal Beach, Calif.

AND

J. H. MOLITOR‡ AND D. MACPHERSON§
Hughes Aircraft Company, Malibu, Calif.

This paper presents the major results from a study of an unmanned asteroid belt probe powered by solar electric propulsion (SEP) and launched by an Atlas/Centaur or a Titan IIIC. The SEP comprises roll-out solar cell arrays, mercury electron-bombardment ion thrusters, and modular solid-state power-conditioning equipment. With a 10-kw solar array (rated at 1 a.u.), the spacecraft would gather information about the flux distribution, size, velocity, and direction of asteroidal and cometary particles as small as 10^{-9} g. The flux data would be accurate to within 10% standard error. The spacecraft would coast in the asteroid belt, between 2 and 3.5 a.u., for almost 1000 days. The trajectory has an aphelion of 3.5 a.u.; thrust is cut off at 210 days, just as the spacecraft reaches 2 a.u.

Introduction

PREVIOUS spacecraft design and mission studies of an asteroid belt mission[1–3] were not as detailed as that[4] from which most of the information in this paper was derived. The two major objectives of the mission are 1) to provide valuable scientific and engineering data about the environment and potential hazards of the asteroid belt region and 2) to demonstrate the applicability and readiness of solar electric ion propulsion (SEP) as a prime propulsion source for unmanned interplanetary exploration. Accordingly, the major study goals were: a) to establish a meaningful and effective mission concept for an asteroid belt survey, b) to develop a minimum-cost SEP spacecraft design and select subsystems and designs compatible with the mission concept, and c) to make maximum use of state-of-the-art technologies. Study guidelines and constraints included use of the Atlas/Centaur or Titan IIIC launch vehicle, use of mercury electron-bombardment ion thruster technology, and use of solar cell arrays of the foldout or roll-out type, with specific weights of 21 and 15 kg/kwe, respectively, with solar power assumed to vary as a function of heliocentric distance, and with a 15% degradation factor for radiation damage.

Selection of the Mission Concept

Selection of the mission concept involved consideration of the possible trajectories, spacecraft sizes, and vehicle configuration tradeoffs. A trajectory with an aphelion of 3.5 a.u. was chosen (Fig. 1), because a spacecraft flying such a trajectory would encounter the maximum number of asteroidal particles. On a trajectory with a larger aphelion, the spacecraft would pass through the most dense region of the asteroid belt very rapidly, encountering particles for only a short time; conversely, for an aphelion under 3.5 A.U., the spacecraft would spend more time traveling in the same general direction as the particles and would not intercept many.

The payload capabilities of a number of thrust-vectoring options were investigated. These options ranged from thrusting continuously normal to the sunline to continuously orienting the vector along the optimum direction while maintaining the solar panels normal to the sunline. The method chosen was to approach the optimum by holding the thrust vector parallel to the plane of the solar arrays and orienting the entire vehicle. During the coast phase, a proper orientation of the vehicle would allow optimization of the encounter geometry between the detectors (mounted on the antisolar side of the solar arrays) and the particles (see Fig. 2).

The selection of a spacecraft design required the careful evaluation of the scientific-payload requirements, which were then compared to the capabilities of the launch vehicle and of the SEP power level. The payload performance capabilities of candidate spacecraft design points (power level, specific impulse, and launch vehicle) were based on the results of trajectory analyses and preliminary subsystem sizing. Since this was the first potential application of SEP for primary thrust on an unmanned exploratory spacecraft, it was desirable to use modest propulsion system input power (P_0) levels. Consequently, P_0 levels (at 1 a.u.) on the order of 4, 6, and 8 kw were considered for the Atlas/Centaur/SEP spacecraft. These power levels indicate total spacecraft power requirements of approximately 5, 7.5, and 10 kw, respectively, when a 15% radiation degradation factor, the spacecraft housekeeping power, and the distribution losses are included. The curves with positive slopes in Fig. 3 show scientific-payload weight capability vs P_0 for the candidate concepts. The data also indicate the variation in the available scientific-payload weights for the specific impulse (I_{sp}) selected. For the

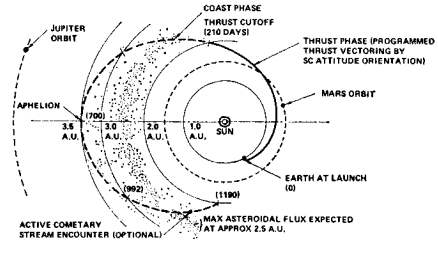

Fig. 1 Recommended mission profile.

Presented as Paper 70-1121 at the AIAA 8th Electric Propulsion Conference, Stanford, Calif., August 31–September 2, 1970; submitted September 24, 1970; revision received January 15, 1971. Most of the information in this paper was derived from a study conducted by North American Rockwell for the Jet Propulsion Laboratory (JPL) under Contract 952566.

* Program Manager, Advanced Programs, Space Division. Member AIAA.
† Member of the Technical Staff, Space Division.
‡ Manager, Ion Physics Department. Member AIAA.
§ Senior Staff Engineer.

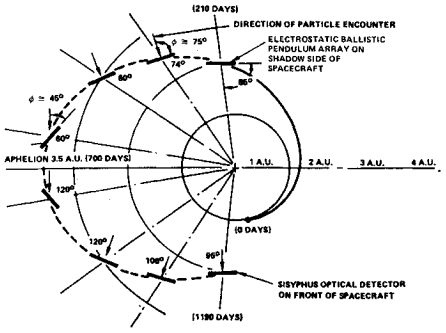

Fig. 2 Spacecraft orientation and direction of asteroidal-particle encounter.

Atlas/Centaur/SEP spacecraft, the decrease in payload capability associated with the use of an I_{sp} of 3500 sec is rather insignificant at the higher power levels compared with those for I_{sp} values closer to optimum.

To obtain a 10% standard error, or better, for data on particles weighing 10^{-7} g, 750 ft² (70 m²) of particle-penetration detectors are required. Table 1 shows that detector weight increases as total spacecraft power decreases, because, for example, a 10-kw solar array has enough substrate area for mounting 750 ft² of detectors, whereas a 5-kw array can accommodate only half this amount. Therefore, for a 5-kw spacecraft, a separate structural array must be provided on which to mount the other half of the required detectors, thus increasing weight.

The two curves with negative slopes in Fig. 3 show the effect of using independent particle-detector panels. For $P_0 <$ 7.75 kw, insufficient area is available on the backside of the solar panels for bonding 750 ft² of detectors. Furthermore, the heavy penalty resulting from the use of independent panels pushes the scientific-payload weight beyond the capability of the spacecraft at lower levels.

As a result of this evaluation, study efforts were concentrated on 10 kw of total power and $P_0 \simeq 8$ kw. A 3500-sec I_{sp} was selected because of the state-of-the-art thruster design and suitability for other potential missions. The Atlas/-Centaur launch vehicle was selected because it has adequate payload capability and lower cost than Titan IIIC. However, the spacecraft designed could be launched with the Titan IIIC because the payload envelopes are very similar (both use 120-in.-diam shrouds), and the Titan IIIC shroud can accommodate various payload lengths by use of 5-ft-long shroud extension cylinders.

Table 1 Scientific-payload requirements

Required detector area = 750 ft² ≥10^{-7}-g particles 10% standard error from 2.4 to 2.6 a.u.		Spacecraft power		
Order - of - magnitude contingency		5 kw	7.5 kw	10 kw
Detectors on back of solar arrays (75% array substrate covered)	Area, m²	35	52	70
	Weight, kg	15.5	23	31
Independent detector arrays	Area, m²	35	18	...
	Weight, kg	63	32.4	...
Total detector	weight, kg	78.5	55.4	31
Sisyphus, electrostatic ballistic pendulum, particle and field experiments	Weight, kg	49	49	49
Total scientific-payload	weight, kg	127.5	104.4	80

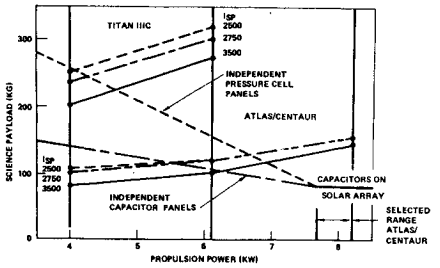

Fig. 3 Science-payload capacity vs requirements.

The need to provide a clear field of view throughout the entire mission for the attitude reference star trackers was a major consideration. Figure 4 shows four approaches that also satisfy the design constraint of keeping all spacecraft appendages forward of the ion-exit plane. In configuration A, use of the star Canopus requires that the solar panels (in the plane of the paper) be deployed forward. For missions in the ecliptic plane, where the ion engines operate throughout most of the mission, this approach is acceptable, since the thrust vector can be used to compensate for solar-pressure disturbance torques resulting from such an arrangement. For missions that involve long coast periods, the inherent large misalignment of the center of pressure and the center of gravity (c.g.) requires a large amount of fuel to compensate for the disturbing torque (~40 kg of GN_2).

For configuration B, the approach is to orient the entire vehicle so that the lower panels are outside the tracker's field of view. The resulting small (<5°) inclination to the ecliptic plane results in an Hg fuel penalty of ~35 kg. In configuration C, only the lower solar panel is canted toward the sun, resulting in an unbalanced, nonsymmetrical configuration. For a modest array weight penalty of 5 kg, configuration C can be designed to accommodate its c.g. location, but length, cell arrangement, and thermal properties for the canted and noncanted arrays differ.

Configuration D uses the sun and two stars, Canopus in the south and Vega in the north, as references. The spacecraft can view one or the other of these stars during any portion of the trajectory, with only 15° of symmetrical canting of the top and bottom solar panels toward the sun. The panels are expected to deflect away from the sun due to the thermally induced bending of the extension boom members. Bending back to the vertical by as much as 5° at 1 a.u. could be expected. Should this occur, a sufficiently clear field of view would still exist for the trackers, and the reference stars would never become obscured. The symmetry of concept D and the cost advantages of using identical solar arrays make it the preferred concept.

For an out-of-ecliptic mission, the position of the Canopus and Vega star trackers must be changed to point forward along the longitudinal axis of the spacecraft, because the unique thrust-vector orientation required for this mission is essentially normal to the orbital plane. Additionally, a second degree of freedom must be incorporated in the high-gain

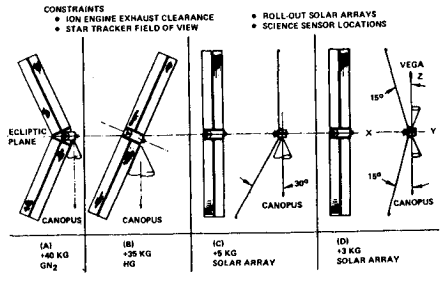

Fig. 4 Evaluation of spacecraft configuration.

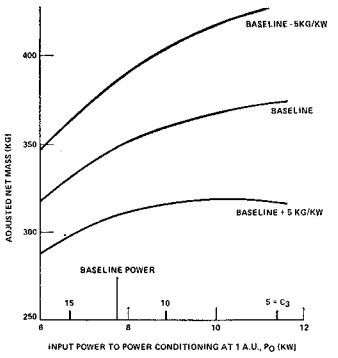

Fig. 5 Effect of change in propulsion system specific mass.

antenna gimbal mount to provide out-of-ecliptic pointing. For an alternative mission, major modifications to the scientific payload would be likely, but this probably would not significantly alter the basic equipment and modular design of the SEP spacecraft.

Trajectory Analysis for Baseline Mission

Parameters defining the baseline spacecraft configuration are I_{sp}, solar panel power and degradation, heliocentric radius at thrust termination, launch vehicle performance, and low-thrust electric propulsion system (EPS) efficiency. Other EPS and trajectory parameters were determined in the optimization process. The value of C_3 for the baseline trajectory is 12.2 $(km/sec)^2$, with a resultant injected mass capability of 751 kg using the Atlas/Centaur.

An I_{sp} of 3500 sec represents proven technology and offers greater versatility for carrying out alternative missions. The performance cost of this choice for the asteroid belt probe is ~20 kg. The solar-panel-rated power of 10 kw is assumed to undergo an 18% degradation upon panel deployment; this power level allows for radiation and asteroidal particle impact damage and for power losses between the solar panels and the power conditioners. Spacecraft housekeeping power of 450 w was deducted from available solar panel power before the thrust was computed.

Low thrust would be terminated at 2 a.u., 210 days into the mission. This decision was based on the desirability of not thrusting while conducting the scientific experiments; most of these are conducted beyond 2 a.u.

In the initial trajectory analysis, the payoff function was assumed to be the net mass, defined as the injected mass less the masses of the solar panels, Hg, and EPS. (The EPS includes the thrusters, power conditioners, propellant tank, and ~16 kg for mechanisms, plumbing, etc.) The proper payoff function, however, is adjusted net mass m_{na}, i.e., spacecraft net mass less those parts of the spacecraft subsystems that would not be needed if the low-thrust EPS were removed. It is this mass that should be considered when making comparisons with ballistic alternatives for carrying out the mission. In most cases, the design recommendations resulting from the analysis would not be changed by using m_{na} rather than net mass as a payoff function. This insensitivity is fortunate, because m_{na} is a function of the actual spacecraft design configuration and, therefore, cannot be reliably estimated in the beginning. The mass breakdown for the baseline spacecraft is shown in Table 2.

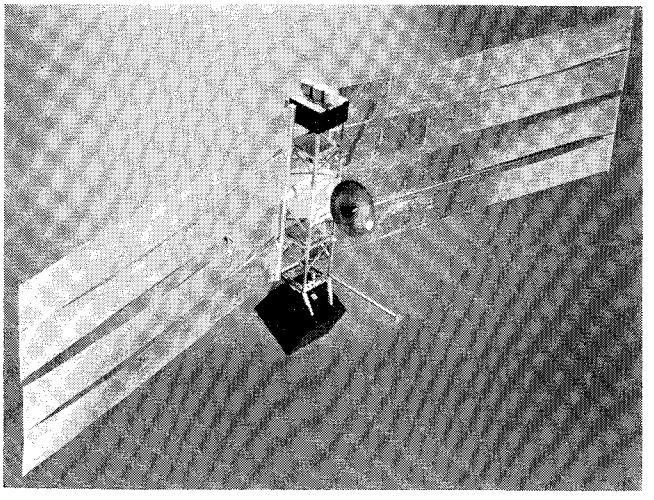

Fig. 6 Recommended spacecraft configuration.

In the following discussion, performance changes due to changes in propulsion system size are assumed to increase or decrease the performance pad rather than to change the subsystem masses.

The power-conditioning (PC) mass was assumed to vary linearly with P_0 (the input power to the power conditioners at 1 a.u.). Solar panel specific mass α_{panel} was assumed to be 15 kg/kwe undergraded (18.3 kg/kwe based on P_0). Since differential changes to the nominal General Electric Company roll-out array design actually occur at somewhat smaller values of α_{panel}, this assumption favors trajectories using lower power EPS's. Note that ~6% of the solar panel is used to generate spacecraft housekeeping power but is charged to the propulsion system to avoid complicating the bookkeeping.

The spacecraft cabling is assumed to be proportional to P_0. For the baseline design, the cabling between the solar panels, power conditioners and thrusters is assumed to weigh 20 kg. Thermal control is used primarily for the scientific and the spacecraft equipment; 2 kg of the thermal control subsystem weight is associated with the EPS. Approximately 75% of the cold gas and tankage (30 kg—the remaining 25% is assumed to be leakage) in the stability and control subsystem is assumed to be linearly dependent upon P_0. The remaining 37 kg covers items that are essentially independent of spacecraft mass: lines, nozzles, and valves.

The solar array support structures are assumed to weigh 22 kg. The propulsion system and propellant tank require little structural support, because loads on them would be supported largely during launch by the payload interstage for the recommended spacecraft design. (In other designs, a larger percentage of the structure may be power-dependent.)

The m_{na} for the baseline trajectory is 350 kg. In Fig. 5, the baseline m_{na} is shown as a function of P_0; thrust for all trajectories would be terminated at 2 a.u. The variations of P_0 in this illustration are the power-level limits used in the

Table 2 Subsystem masses[a]

Subsystem	Mass kg	Mass lb	% of Total
Scientific payload	80	176	11
Electric propulsion	62.5 (62.5)	138	23
Propellant	107 (107)	236	
Solar panels	155 (155)	341	21
Communications and data handling	61	135	45
Central computer and sequencer	10.5	23	
Spacecraft power	28.5	63	
Cabling	54.5 (20)	120	
Thermal control	14.5 (2)	32	
Stabilization and control	77 (30)	170	
Structure	77 (22)	170	
Total	727.5 (398.5)	1604	100
Atlas/Centaur capability $C_3 = 12.2$ $(km/sec)^2$	751	1656	
Contingency	23.5	52	

[a] Numbers in parentheses are propulsion-power-dependent masses.

present design. Preliminary studies showed that the optimum performance trajectory has a P_0 value slightly more than 12 kw ($C_3 \simeq 3$ km^2/sec^2), but the theoretical performance improvement in going from 10 kw to 12 kw is too small to justify the necessary growth in size of the EPS. For $P_0 < 7$ kw, the reduced solar panel area would not accommodate the capacitors deployed on the back of the panel. At present, the 7.75-kw value chosen for the baseline trajectory offers a performance pad of ~20 kg, even though conservative mass estimates have been used. An additional 20 kg could be obtained, if necessary, by increasing P_0 to ~10 kw; on the other hand, reduction in P_0 should not be seriously considered. Variations of ±5 kg/kw from the baseline would affect the adjusted net mass considerably, but the baseline P_0 would still be well below the "optimum" power.

It must be emphasized that any attempt to "optimize" the scientific payload directly is unsound, because small payload numbers are obtained by subtracting relatively large assumed subsystem masses from the total injected mass; thus, computed payload is very sensitive to the assumed subsystem mass scaling.

Design Considerations

Both roll-out and foldout types of solar cell arrays were considered, with specific masses of 15 and 21 kg/kw, respectively. The bonding of capacitor-type particle-impact detector sheets on the antisolar side of the roll-out arrays was found to raise their temperature only 7°, which results in negligible power loss. Since the lighter roll-out arrays also require less stowage space, and no significant advantages were identified for the foldout arrays, the roll-out arrays were chosen.

The entire spacecraft would be maneuvered to orient the thrust vector during the thrusting phase, rather than using vectorable thrusters, because the weight and complexity penalties of a spacecraft designed to accommodate the latter while maintaining the solar panels always normal to the sun are greater than the theoretical increase in performance. Consequently, a fixed solar panel/spacecraft bus concept was adopted. The spacecraft would make almost one complete revolution around the sun, and a rigidly mounted tracker would detect a reference star in the south or north celestial sphere as a point moving in a circular pattern at times obscured by the solar panels. By using dual trackers as previously noted, each tracker can view either Canopus (south) or Vega (north) during any portion of the trajectory (Figs. 4D and 6).

For the recommended configuration a mass distribution analysis has defined the c.g. offset problem resulting from the 15° canted solar arrays and the location of scientific equipment, and a preliminary structural analysis has been completed. One pair of solar cell arrays is mounted on a rotatable base to permit reorientation away from the sun after aphelion passage, thus maintaining the capacitor sheets on this pair in the proper geometry for asteroidal particle encounter during coast back to 2 a.u.

The compartmental structural approach (Fig. 7) simplifies manufacture, test, checkout, and design changes. The electric propulsion module, equipment compartment, and scientific payload section are designed as separate entities. Each can be checked out without being physically attached to the others. The solar array power bus is in the equipment compartment, and the arrays are mechanically attached to the sides of the three structural modules. After being checked out individually, the three modules are mated, and the final integration tests and checkout operations are conducted. The four longerons of each module are aluminum angle, and the diagonals are aluminum tees. Mechanical fasteners are used for these members, for the equipment supports, and for mating the modules, to minimize tooling and costs.

Most of the equipment for experiments is mounted on the antisolar side of the science module. Three meteoroid experiments are involved. The particle-penetration detector sheets are bonded to the substrate of the roll-out solar arrays. There are 7 modules of electrostatic ballistic pendulums with a 60° square field of view. One meteoroid sensor is the Sisyphus optical detector, whose very narrow field of view (2°), large size, and pointing requirements make it an important factor in the design of the payload section. It is pointed away from the sun and nearly normal to the direction of particle encounter.

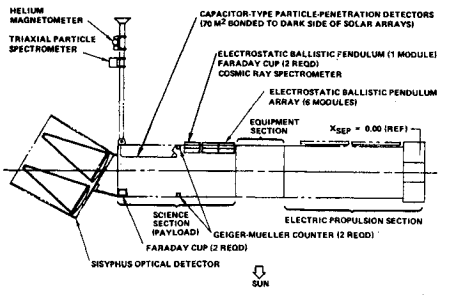

Fig. 7 Location of scientific equipment.

Sensors are provided for five field and particle experiments. The helium magnetometer requires no specific orientation, but its orientation must be known at all times. Since it must be isolated from the spacecraft, it is mounted on the tip of the antisolar low-gain antenna boom. The triaxial particle spectrometer must have an unobstructed 10° conical field of view in three orthogonal directions. One of the sensor elements points away from the sun, the second is normal to the ecliptic plane, and the third points forward, parallel with the spacecraft's longitudinal axis. This instrument also is mounted on the low-gain antenna boom. The four Faraday cups have 45° conical fields of view; two are oriented toward the sun, two away from it. The two Geiger-Mueller counters have 90° fields of view: one faces the sun, the other away from it. The fifth sensor is a cosmic ray spectrometer with a 60° conical field of view.

The equipment compartment, which is 1 m square and 0.9 m long, provides hard points for the attachment of the high-gain antenna support truss and the rollout solar array end-support fittings. Twelve cold gas (GN_2) stabilization and control jets are mounted on the periphery of the compartment equidistant from the longitudinal axis at the coast-phase c.g. position. The surface that faces away from the sun is covered with ~0.76 m^2 of thermal-control louvers. Two 36-cm-diam spherical GN_2 tanks are mounted on cylindrical support skirts along the longitudinal axis. Subsystem electronic equipment is mounted on the antisolar side of the compartment, so that, after the solar arrays are deployed and the mercury fuel is expended, the c.g. of the spacecraft is coincident with the center of solar pressure, and the equipment position facilitates thermal control. Inside surfaces of the equipment compartment, except the louvered side are insulated with 25 layers of aluminized Mylar. The external surface is covered with meteoroid bumper skin. For a 90% probability of no meteoroid damage, the total thickness of the insulation, the bumper skin, and the compartment outer skin should be 3 mm; the thicknesses chosen are 0.75, 0.75, and 1.5 mm, respectively.

The louvered side of the equipment compartment is provided by a unique bumper concept. Equipment within the compartment is mounted on a structural shear plate, which also serves as a thermal radiator. This plate, which faces the louvers, provides the second sheet of protection for the equipment. It is 3 mm thick—a value determined from an analysis of meteoroid damage (the ratio of outer-sheet to inner-sheet thickness must be 0.25). The outer bumper consists of an aluminum screen with ~50% open area. The closed area does not increase the louver area by the same percentage, however; only a 33% increase in total louver area is required.

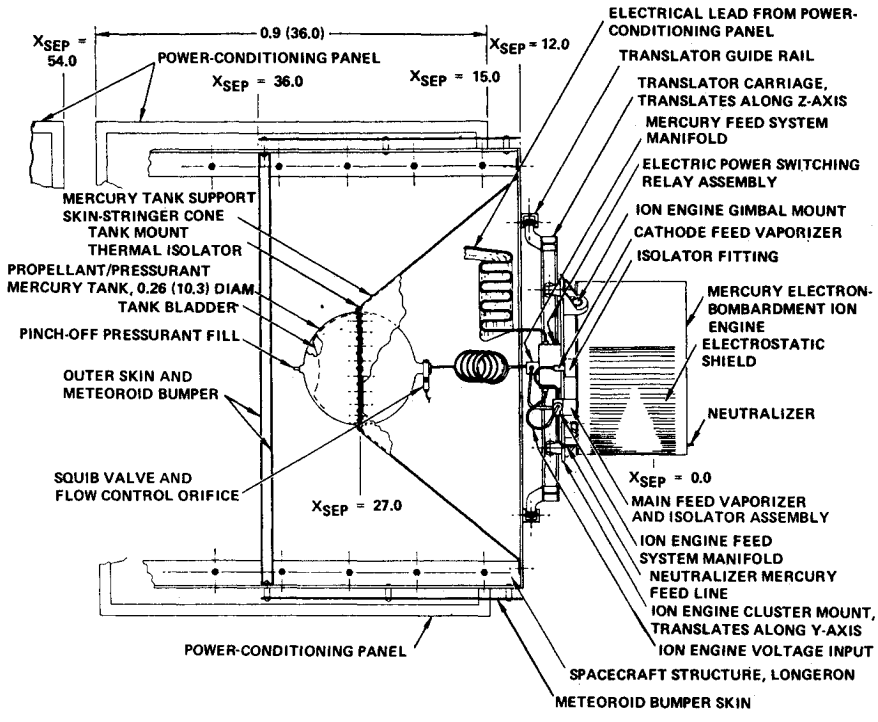

Fig. 8 Electric propulsion module.

The compartment is designed to permit equipment removal from the louvered side.

The EPS module's structure is similar to that of the payload section (Fig. 8). An enclosed portion forward of the ion engines houses the tankage and electrical and propellant feed systems. The structure provides hard points for the central mounting of fitting and end supports for two of the roll-out arrays. The ion engines are attached to the module structure through a dual-axis linear translator. Two PC panels are attached with thermal-isolation mounts to the shaded external part of the structure. They are shielded on the sun-facing side by eight layers of aluminized Mylar insulation and an aluminum bumper sheet, and on the radiating side by a bumper sheet; both surfaces have thermal-control coatings. Internal heaters keep the panels within allowable temperature limits during nonoperating periods.

The 25.2-cm-diam Hg propellant/pressurant tank, which is mounted on a conical skin stringer support, is located on the longitudinal axis to minimize c.g. shifts resulting from the use of propellant. A squib valve and flow-control orifice on the aft end of the tank prevent the possible hammering of the thruster vaporizer screens by the liquid mercury during launch. Power for the engines enters the switching network, attached to the translator, which directs it to the operating engine or engines. A double skin protects the compartment against meteoroids. The EP equipment is sufficiently protected so that it would be possible to restart the thrusters at the end of the mission to provide data on the system's survivability.

Each thruster is attached to hinge ($\pm 10°$) mounts to provide attitude about the longitudinal (X) axis during two-thruster operations. The hinge mounts are attached to the engine cluster mount by thermal isolators. The engine cluster mount translates ± 8 cm along the Y axis and ± 43 cm along the Z axis (see Fig. 4D). Both the cluster mount and carriage are driven by stepper motor-gear reduction units. The mount and carriage are guided by self-aligning, V-groove rollers at four points on each structure.

Two candidates were investigated as electrical power feeds to the thrusters across the translator: a flat "ribbon" wire design and the common round cable. The former, which incorporates a loop-upon-loop approach to accommodate the translation motion, minimizes weight and more efficiently dissipates heat.

Electric Propulsion System

The EPS not only provides the energy for the heliocentric transfer trajectory but also constitutes the major technological experiment. The design points are: solar panel power at 1 a.u., 7.75 kw; solar panel bus voltage at 1 a.u., 40 v; Hg mass, 107 kg; I_{sp}, 3500 sec; and trajectory as shown in Fig. 1. The thruster array includes three 3.62-kw thruster modules, one of which is a standby. Thrusting begins with two thrusters operating at their nominal power. As the mission progresses, the solar array power decreases, and the Hg flow rate and the resultant beam current are decreased (at constant voltage) until the total beam power output of the two thrusters is equal to the beam power that one thruster would deliver if run at full power. At this point (134 days), one thruster is shut down and one is brought back to full power. This operating thruster is throttled to match the available solar array power until the end of the thrusting period (210 days).

Two PC panels are provided, one for each operating thruster. If a thruster fails during the mission, the standby thruster is connected to the PC panel of the failed thruster by a switching matrix. Since there are no standby panels, PC redundancy is built into each panel. Because of the extreme penalty additional propellant imposes, redundancy in the Hg reservoir system is undesirable.

Each thruster has three propellant vaporizers and two high-voltage isolators. Two of the vaporizers supply Hg vapor to the hollow cathodes employed in the discharge chamber and neutralizer, while the third controls the main flow to the discharge chamber. The two isolators, located in the feed lines to the discharge chamber, electrically isolate the Hg reservoir from the high-voltage thruster. Each 40.7-cm-diam $\times$ 26.9-cm-long thruster module weighs 4 kg and has a total efficiency of 72%, a thrust level of 37.5 g, and an input power of 3.6 kw. The Hg reservoir pressure is controlled at 22 atm.

Each 30-cm-diam thruster nominally requires $\sim$3.62 kw of conditioned power, from low a.c. voltage to high d.c. voltage, regulated for the wide variation of solar array voltages, and controlled over large ranges to maintain and vary thrust. Each PC panel has a 3.9 kwe is capability. For high efficiency, low weight, and long-term reliability, a modular-inverter technique has been developed. Electrically and mechanically discrete, intermediate-power inverters (300 to 500 w) are connected to provide power in the multikilowatt range.

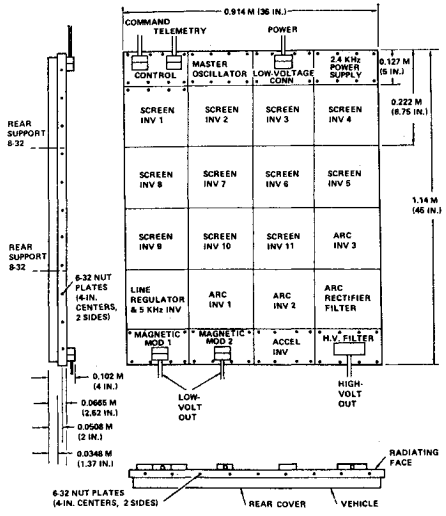

Fig. 9 Layout of power conditioning panel.

Figure 9 delineates the layout of a power-conditioning and control (PC&C) panel. Based on experience with similar systems, the following performance is anticipated for solar array voltages from 40 to 80 v: mass—15–16 kg; efficiency—90 to 91%; reliability—0.96 for 10,000 hr; regulation—±1% on outputs for 40- to 80-v line; control—±1% of command value on outputs; telemetry:—5 v full scale, 10 kw-ohm source impedance, ±2% on full scale on all measured parameters, ±1% over limited range; commands—28 v, 10 ma, 20-msec pulse into latching relays for PREHEAT, LOW-VOLTAGE ON, HIGH-VOLTAGE ON, OFF; 0–5 v, 10-kw load for screen current command

Figure 10, a functional schematic of the SEP system, shows its interface with the spacecraft stabilization and control subsystem. The navigation and guidance functions are performed on the ground; the computations yield the desired thrust acceleration magnitude and orientation programs. The thrust acceleration magnitude is controlled by direct commands for the thruster and PC ON/OFF switching and beam current. (Logic is included to protect the EPS in the event of thruster failure or other malfunction). Thrust vector control to satisfy the commanded attitude is obtained by on-board computation. Available solar panel power is continuously examined by the peak-power monitor, and beam current I_B is regulated by closed-loop control. If adequate solar panel power is available, the value requested from the thrusters (I_{BR}) is identical to the command (I_{BC}). If I_{BC} can not be provided, I_{BR} is commanded to be the maximum attainable value.

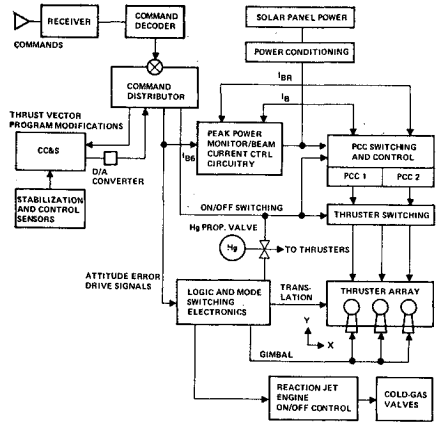

Fig. 10 SEP system interface with stabilization and control system.

Concluding Remarks

The asteroid belt could be effectively surveyed by an unmanned SEP spacecraft launched by an Atlas/Centaur vehicle. The 10-kw spacecraft described herein is believed to be the simplest and least costly configuration that present technology can produce. Besides roll-out solar cell arrays, to the backs of which are bonded 75 m² of particle-penetration detectors, its design incorporates separate modules for the propulsion system, the spacecraft equipment, and the scientific payload—an approach that minimizes the interfaces between the propulsion system and the rest of the spacecraft. Since the propulsion system is essentially independent of the other spacecraft modules, including the scientific payload, it could be readily adapted to other missions.

References

[1] Molitor, J. H., Schwaiger, L. E., and MacPherson, D., "Spacecraft Design for Multipurpose Solar Electric Propulsion Missions," *Journal of Spacecraft and Rockets*, Vol. 6, No. 11, Nov. 1969, pp. 1285–1290.

[2] Wrobel, R. W. and Kerrisk, D. N., "Early Exploration of the Asteroid Region by Solar Powered Electrically Propelled Spacecraft," Joint National Meeting American Astronomical Society, Paper XA4, June 17–20, 1969, Denver, Colo.

[3] "Solar Electric Multi-Mission Spacecraft Study," JPL Contract 952394, Feb. 1970, TRW Inc., Redondo Beach, Calif.

[4] "Solar Electric Propulsion Asteroid Belt Mission Study," SD 70-21-1, -2, Jan. 1970, Space Div., North American Rockwell Corp.